

Figure S1. EDX images of: a) Au-Si NCs, b) Au-SiC NCs, c) Au-Ge NCs.

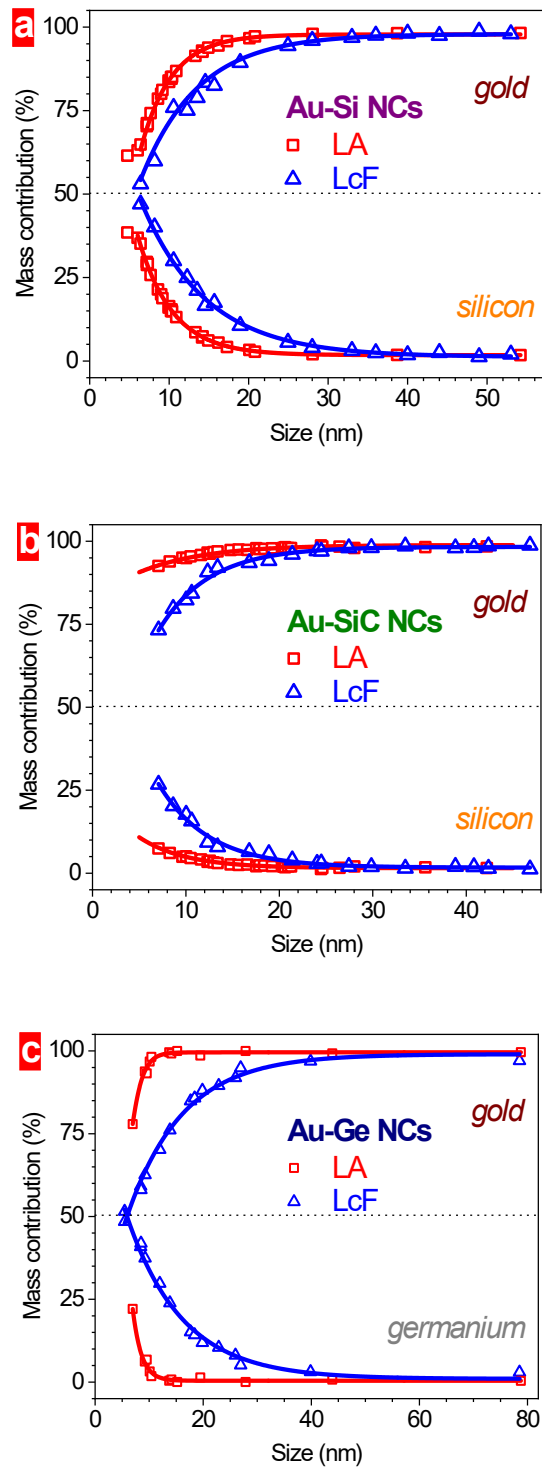


Figure S2. Size-dependent mass contribution of different elements in metallic-semiconductor nanocomposites: a) Au-Si NCs; b) Au-SiC NCs; c) Au-Ge NCs.

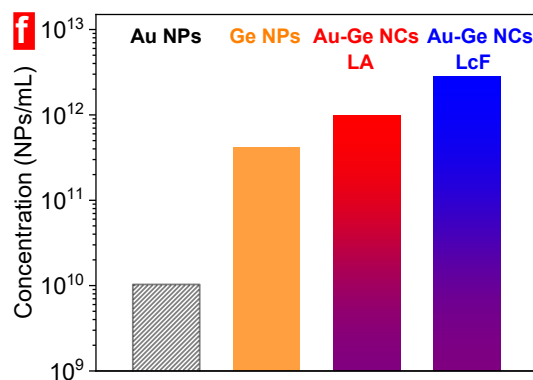
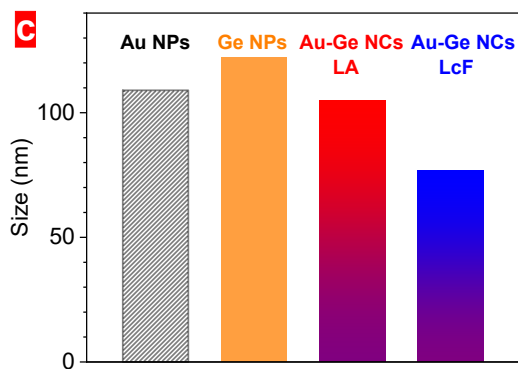
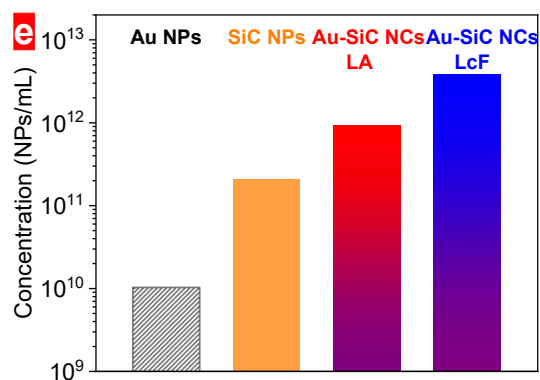
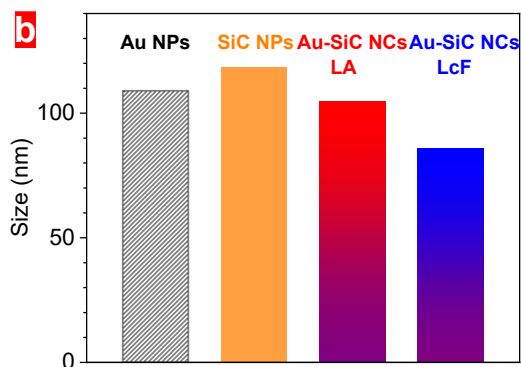
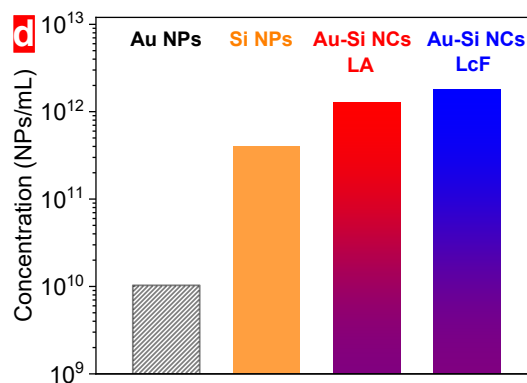
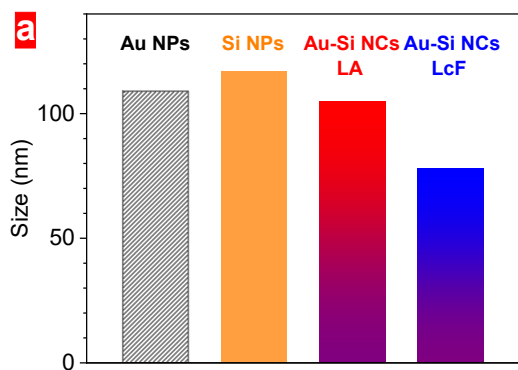


Figure S3. Hydrodynamic size (a-c) and particle concentration (d-f) of metallic-semiconductor NCs as compared to corresponding single-element NPs.

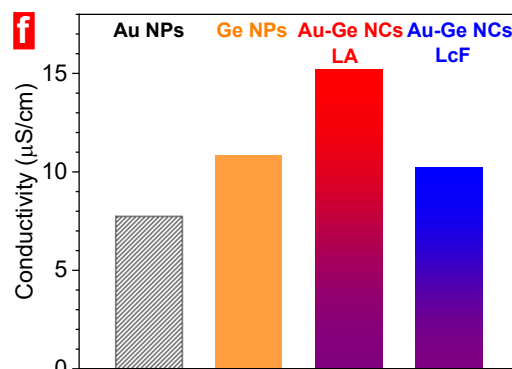
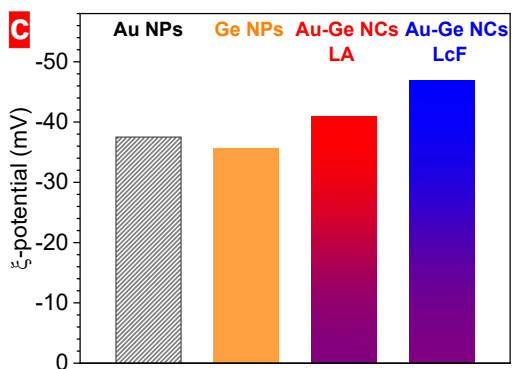
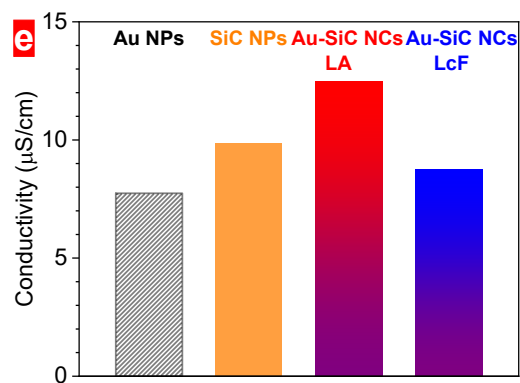
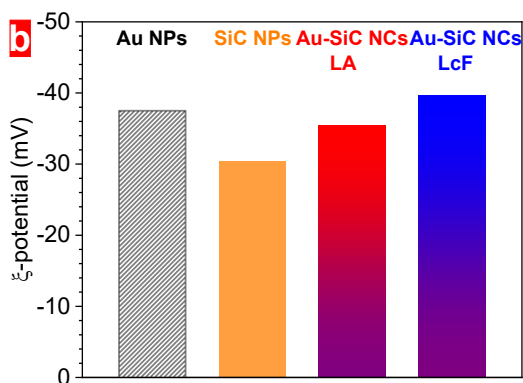
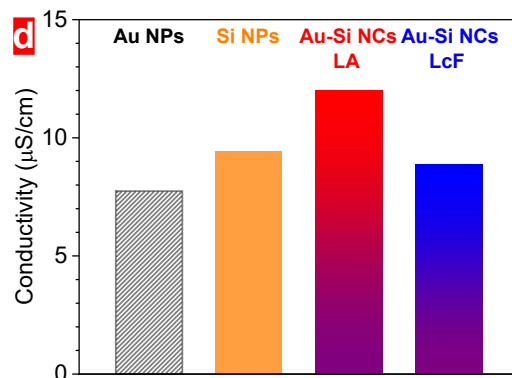
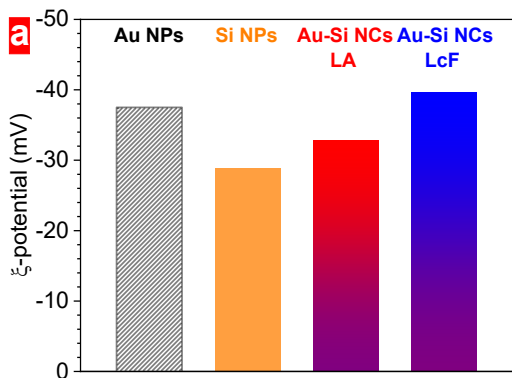


Figure S4.  $\zeta$ -potential (a-c) and electrical conductivity (d-f) of metallic-semiconductor NCs as compared to corresponding single-element NPs.

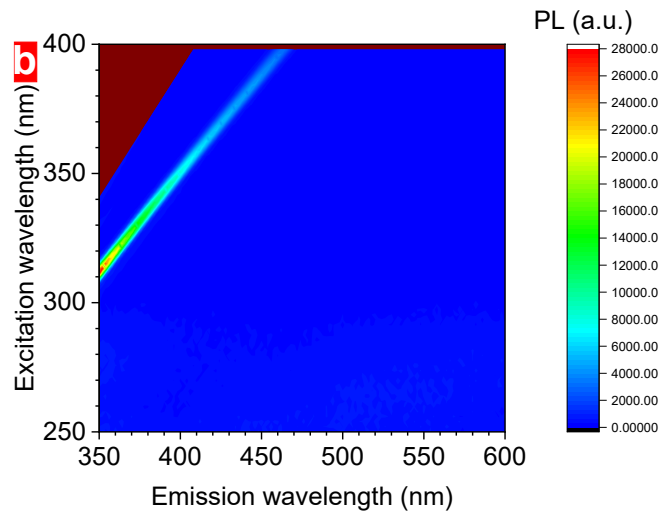
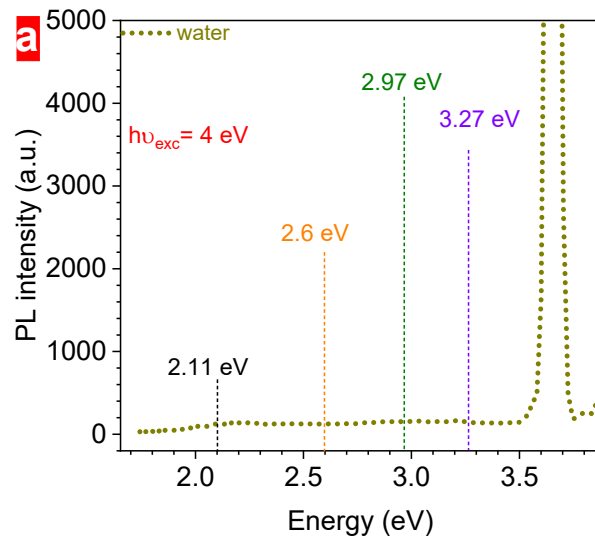


Figure S5. a) PL spectrum and b) mapping of pure deionized water.

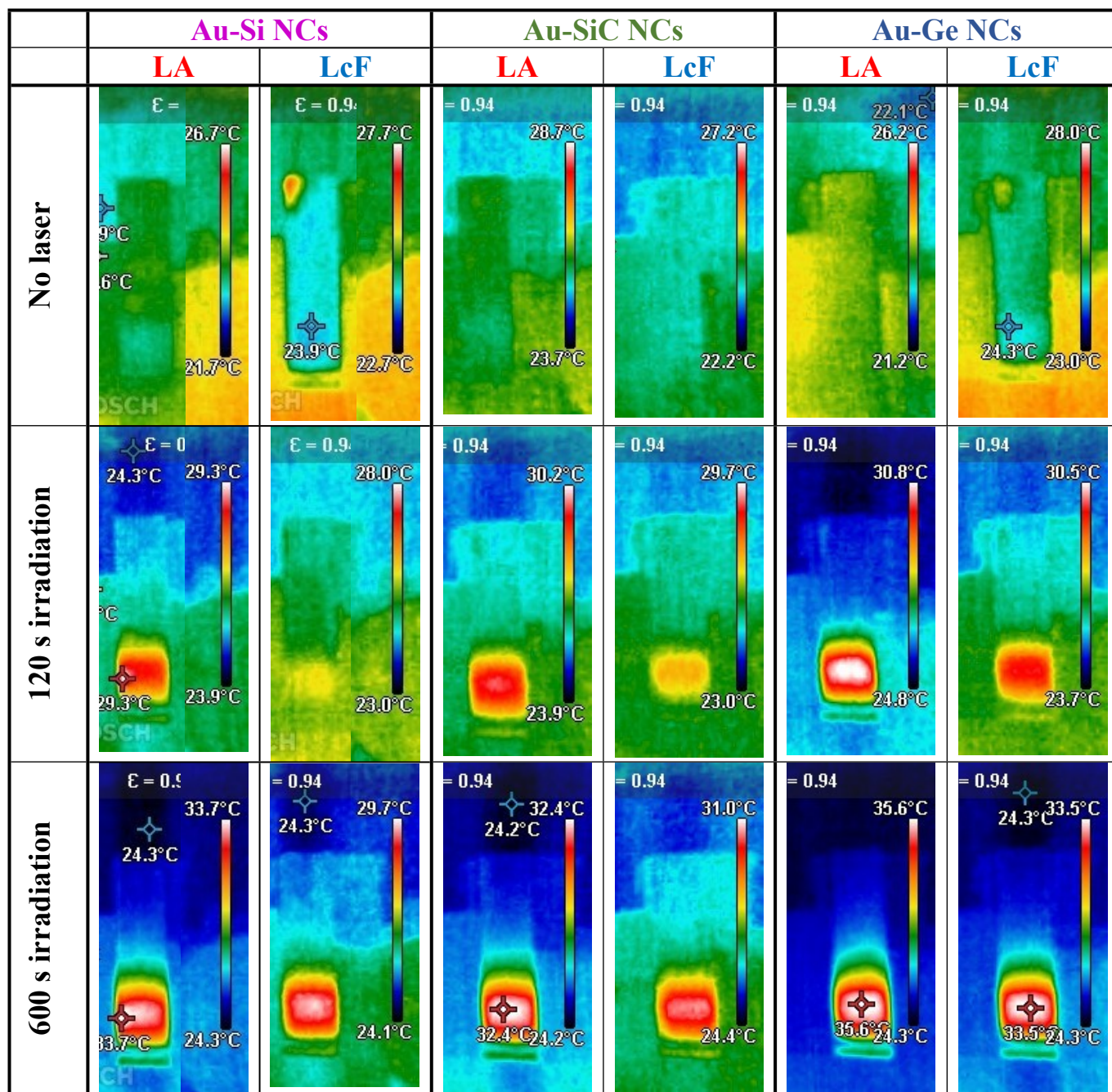


Figure S6. Ultrafast laser-induced heating images of Au-Si NCs, Au-SiC NCs and Au-Ge NCs formed by LA and LcF approaches.